

# Directed Single Beam Transmission of Flat-shaped Visible Light Using Galilean Telescoping Beam Shaper for Scatter Prone Underwater Channels

Tomoya Ishikawa, Ayumu Kariya, Fumiya Kobori, Keita Tanaka, Takahiro Kodama

Faculty of Engineering and Design, Kagawa University, 2217-20 Hayashi-cho, Takamatsu, 761-0396, Japan, [kodama.takahiro@kagawa-u.ac.jp](mailto:kodama.takahiro@kagawa-u.ac.jp)

**Abstract** *We demonstrate through experimentation that shooting a receiving condenser lens with a flat-shaped beam generated from a transmissive telescopic beam shaper can improve the efficiency of the receiving beam of a 405-nm flexible time-domain hybrid PAM signal comprising PAM2 and PAM4 signals in underwater channels. ©2023 The Authors*

## Introduction

In next-generation mobile communication standards, such as beyond 5G/6G, optical wireless communication is a promising candidate for situations requiring significant capacity required. Therefore, research on devices and systems suitable for this purpose is essential [1-5]. Additionally, there is a need to expand the application range of new wireless communication technology by utilizing optical wireless communication for non-terrestrial networks (NTN) [6,7].

One example of NTN is underwater communication networks, and it is necessary to consider long-distance and large-capacity underwater wireless communication systems in anticipation of the introduction of underwater Internet of Things terminals in the future [8]. Visible-light lasers are capable of long-distance, large-capacity communication with minimal propagation delays, making them suitable for underwater optical wireless systems [9]. However, even if a visible band with a relatively small loss is selected, losses caused by the effects of photon absorption and scattering on water molecules cannot be avoided. In the deep sea, where turbidity is relatively low, the scattering coefficient of the medium is small; therefore, blue light is best in the visible light band in terms of low loss in pure water [10]. A time-domain hybrid pulse amplitude modulation (TDHP) scheme was reported to maximize the transmission rate based on the distance in an underwater channel [11].

Wavelength and beam selectivity are essential for long-distance transmission through underwater channels in optical wireless systems. The width of a standard collimated Gaussian beam tends to increase, starting from the beam waist, as the propagation distance increases [12]. Although it is sufficient to increase the beam-cross-section on the receiver side, there is a limit

to increasing the cross-sectional area of each element, such as the condenser lens and the photodetector, considering the overall size of the receiver. Recently, because the beam shape is highly resistant to turbulence, underwater channel transmission shaped into a nondiffractive beam using a spatial phase modulator has been reported [13]. However, because the spatial phase modulator used for beam shaping is an externally inserted active optical device, it increases the power consumption during system operation. Analytical results have shown flat beams are excellent for use when there is turbulence in the water [14]. Recently, uncoupled [15] and coupled [16] flat-top beams with multiple outputs were reported.

In this study, we experimentally demonstrated the propagation characteristics of a flat beam generated by a single light-based transmissive beam shaper as a telescope of Galilean type comprising a passive optical device targeting an underwater channel with high scattering. Compared to other beam-shaping methods, such as a transmissive telescopic beam shaper has the advantages of high efficiency, being independent of wavelength, and zero power consumption. We compared the transmission characteristics of the TDHP signal for three beams (flat, mountain, and valley) generated by a transmissive telescopic beam shaper. To the best of our knowledge, this is the first experimental verification of a receiver-side focusing lens shooting using a transmissive telescopic beam shaper in a highly scattered underwater channel.

## Principle of beam shaping by transmissive telescopic beam shaper

Figures 1(a-c) show the flat, mountain, and valley-shaped beams generated by the transmissive telescopic beam shaper from a collimated Gaussian-shaped input beam. To perform beam shaping with excellent power efficiency, we used the Galilean method, which

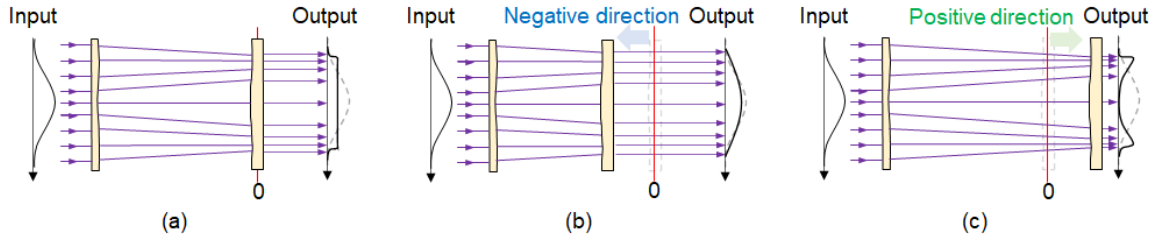


**Fig. 1.** Lens placement setting for transmission telescopic beam shaper: (a) flat-shaped beam case, (b) Gaussian curve-shaped (mountain-shaped) beam case, (c) inverse Gaussian/concave (valley-shaped) beam case.

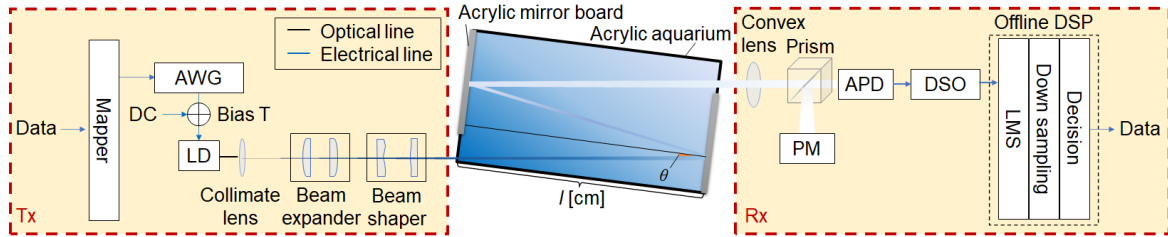


**Fig. 2.** Experimental setup for underwater channel transmission.

re-splits the laser intensity using a field-mapping phase element, such as an aspherical lens. A flat beam was generated by diffusing the central power (at the time of input) to both ends by arranging the aspherical lens in the latter stage at the optimum position (referred to as the 0 points hereafter). A Gaussian curve-shaped (mountain-shaped) beam is generated as an intensity distribution relatively close to a Gaussian distribution by placing an aspherical lens in the negative direction from the 0 points. By arranging the aspherical lens in the positive direction from the 0 points, the inverse Gaussian/concave (valley-shaped) beam had a more substantial intensity distribution at the edge of the beam than that at the center.

### Experimental Setup

Figure 2 shows an experimental system for the underwater channel transmission of a TDHP signal beam shaped by a transmissive telescopic beam shaper. On the transmitter side, a 312.5 Msymbol/s TDHP signal was output from an arbitrary waveform generator (AWG), with a sampling rate of 1.25 Gsample/s and a bandwidth limit of 250 MHz. The TDHP signal is added to a direct current (DC) component and directly modulated by a semiconductor laser diode (LD). The central wavelength of the LD was 405 nm, which is the wavelength of violet light. In this evaluation, a TDHP (1:0) signal composed of pure PAM2, a TDHP (0.5:0.5) signal composed of half PAM2 and half PAM4, and a TDHP (0:1) signal composed of pure PAM4 were used. In  $(x, y)$ ,  $x$  and  $y$  correspond to the PAM2 and PAM4 ratios for all symbols. A collimator converts the Gaussian beam output from the LD into parallel light. The optical power after the collimator output is 0 dBm. After expanding the beam size while

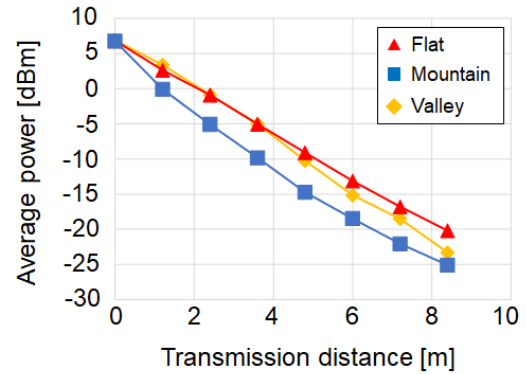


**Fig. 3.** Optical power versus transmission distance.

maintaining a similar light intensity with a beam expander, a flat beam, mountain beam, and valley beam were selected by the beam shaper and output to the underwater channel. The lens adjustment condition of mountain- and valley-shaped beam generation is -10 mm and +10 mm based on the distance between the aspheric lenses that generate flat-shaped beam. The insertion loss of the beam shaper was 0.3 dB.

For the underwater channel, an acrylic tank of dimensions 0.45 m  $\times$  1.2 m  $\times$  0.6 m  $\times$  0.01 m (height  $\times$  length  $\times$  width  $\times$  thickness) is filled with tap water, and a mirror is placed on the side of the tank to reflect multiple times for transmission. On the receiver side, after the beam is incident onto the condenser lens, the beam splitter splits the focused beam. The condenser lens diameter was 25.4 mm. The received power of the subbeam was monitored using a power meter (PM). The main beam is received by an avalanche photodetector (APD) and converted into electrical signals. The electrical signal is sampled and quantized using a digital storage oscilloscope (DSO) at a sampling rate of 2.5

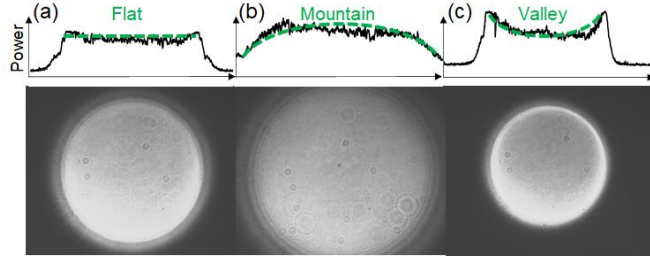


Fig. 4. Beam cross-section image: (a) flat, (b) mountain, (c) valley.

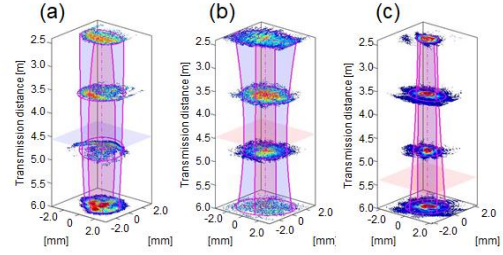


Fig. 5. Beam profiles: (a) flat, (b) mountain, (c) valley.

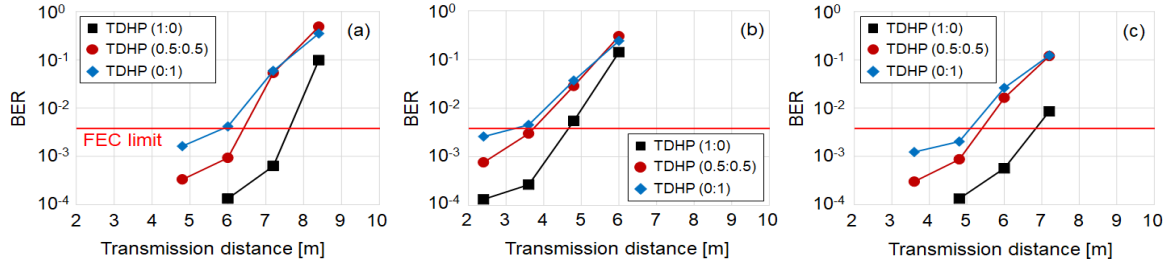


Fig. 6. Experimental BERs for transmission distance: (a) flat, (b) mountain, (c) valley.

Gsample/s and a bandwidth limit of 300 MHz. In offline digital signal processing (DSP) on the receiver side, after compensating for the band limitation of the radio frequency device using time-domain equalization using the least-mean-square (LMS) algorithm, the original data stream is restored by hard decision processing.

### Experimental Results

Figure 3 shows the optical power of the underwater channel versus the transmission distance for the flat, mountain, and valley-shaped beams. The flat beam had lower energy than the other two, regardless of the transmission distance. Valley-shaped beams exhibited greater power attenuation than flat-shaped beams with increasing distance.

Figures 4(a-c) show images of the beam cross-sections and intensity distributions of the flat, mountain, and valley-shaped beams (acquired by the camera) before transmission through the underwater channel after beam shaping. We can confirm that all the beam shapes are based on the principle depending on the setting of the lens.

Figures 5(a-c) compare beam profiles for transmission distances up to 8 m. We can confirm that the flat beam maintains high-intensity power at its center. We ensured that the mountain-shaped beam was wide at the initial transmission stage and spread out as the distance increased. The beam spread of the valley-shaped beam was small for the given space, but the beam spread at 6 m was more significant than that of the flat-shaped beam.

Figures 6(a-c) compare the bit error ratio (BER) characteristics of the three types of TDHP signals for transmission distances of up to 8 m. This can extend the distance to reach the forward error

correction (FEC) limit by reducing the transmission rate of the TDHP signal. Because it is assumed that the Reed-Solomon RS (255,239), a hard-decision FEC, is used, the error correction limit is  $BER = 3.8 \times 10^{-3}$ . The TDHP (1:0), TDHP (0.5:0.5), and TDHP (0:1) transmission distances at the FEC limit of the flat beam were 7.6 m, 6.4 m, and 5.8 m. The TDHP (1:0), TDHP (0.5:0.5), and TDHP (0:1) transmission distances at the FEC limit of the mountain beam were 4.6 m, 3.7 m, and 3.2 m. The TDHP (1:0), TDHP (0.5:0.5), and TDHP (0:1) transmission distances at the FEC limit of the valley beam are 6.8 m, 5.4 m, and 5.1 m. Therefore, we can see that flat beams can transmit over long distances for any TDHP signal. In addition, we verified that adaptive modulation using the TDHP can change the maximum transmission distance.

### Conclusions

Considering a receiving condenser lens placed in an underwater channel, a proof-of-principle experiment revealed that the TDHP signal of a flat beam with good beam power efficiency generated by a transmissive telescopic beam shaper has superior BER characteristics compared to the mountain and valley-shaped beams. In tap water channel transmission using TDHP signal with a flat-shaped single beam with a low transmission power of 6 dBm, we showed that the transmission capacity of 312.5 to 625 Mbps distance could be adaptively transmitted over a transmission distance of 5.8 to 7.6 m. In future research on flat beams, we will study long-distance transmission with increased transmission beam intensity and communication in highly turbid underwater channels.

## References

- [1] P. K. Singya, B. Makki, A. D'Errico, and M. S. Alouini, "Hybrid FSO/THz-based backhaul network for mmWave terrestrial communication," *IEEE Transactions on Wireless Communications*, Dec. 2022. DOI: [10.1109/TWC.2022.3224331](https://doi.org/10.1109/TWC.2022.3224331)
- [2] S. Ishimura, R. Morita, T. Inoue, K. Nishimura, H. Takahashi, T. Tsuritani, M. D. Zeysa, K. Ishizaki, M. Suzuki, and S. Noda, "Proposal and demonstration of free-space optical communication using lens-free photonic-crystal surface-emitting laser," *Proc. European Conference on Optical Communication (ECOC)*, Th3A.7, Sept. 2022.
- [3] T. Koonen, K. A. Mekonnen, Z. Cao, F. Huijskens, N. Q. Pham, and E. Tangdionga, "Beam-steered optical wireless communication for industry 4.0," *IEEE Journal of Selected Topics in Quantum Electronics*, vol. 27, no. 6, Nov.-Dec. 2021. DOI: [10.1109/JSTQE.2021.3092837](https://doi.org/10.1109/JSTQE.2021.3092837)
- [4] M. Hinrichs, P. W. Berenguer, J. Hilt, P. Hellwig, D. Schulz, A. Paraskevopoulos, K. L. Bober, R. Freund, and V. Jungnickel, "A physical layer for low power optical wireless communications," *IEEE Transactions on Green Communications and Networking*, vol. 5, no. 1, Mar. 2021. DOI: [10.1109/TGCN.2020.3038692](https://doi.org/10.1109/TGCN.2020.3038692)
- [5] Z. Hu, Z. Chen, Y. Li, D. M. Benton, A. A. I. Ali, M. P. atel, M. P. J. Lavery, and A. D. Ellis, "Adaptive Transceiver Design for High-capacity Multi-modal Free-space Optical Communications with Commercial Devices and Atmospheric Turbulence," *IEEE Journal of Lightwave Technology*. DOI: [10.1109/JLT.2023.3242215](https://doi.org/10.1109/JLT.2023.3242215)
- [6] C.W. Chow, C. H. Yeh, Y. Liu, Y. Lai, L. Y. Wei, C. W. Hsu, G. H. Chen, X. L. Liao, and K. H. Lin, "Enabling technologies for optical wireless communication systems," *Proc. Optical Fiber Communication Conference (OFC)*, M2F.1, Mar. 2020.
- [7] K. Wang, T. Song, Y. Wang, C. Fang, J. He, A. Nirmalathas, C. Lim, E. Wong, and S. Kandeepan, "Evolution of short-range wireless communications," *IEEE Journal of Lightwave Technology*, vol. 41, no. 4, pp. 1019-1040, Feb. 2023. DOI: [10.1109/JLT.2022.3215590](https://doi.org/10.1109/JLT.2022.3215590)
- [8] P. A. Hoehner, J. Sticklus, and A. Harlakin, "Underwater optical wireless communications in swarm robotics: A tutorial," *IEEE Communications Surveys & Tutorials*, vol. 23, no. 4, pp. 2630-2659, Fourthquarter 2021. DOI: [10.1109/COMST.2021.3111984](https://doi.org/10.1109/COMST.2021.3111984)
- [9] H. Kaushal and G. Kaddoum, "Underwater Optical Wireless Communication," *IEEE Access*, vol. 4, pp. 1518-1547, 2016. DOI: [10.1109/ACCESS.2016.2552538](https://doi.org/10.1109/ACCESS.2016.2552538)
- [10] J. Shi, X. Zhu, F. Wang, P. Zou, Y. Zhou, J. Liu, F. Jiang, and N. Chi, "Net data rate of 14.6 Gbit/s underwater VLC utilizing silicon substrate common-anode five primary colors LED," *Proc. Optical Fiber Communication Conference (OFC)*, M3I.5, Mar. 2019 DOI: [10.1364/OFC.2019.M3I.5](https://doi.org/10.1364/OFC.2019.M3I.5)
- [11] T. Kodama, M. A. B. A. Sanusi, F. Kobori, T. Kimura, Y. Inoue, and M. Jinno, "Comprehensive Analysis of Time-Domain Hybrid PAM for Data-Rate and Distance Adaptive UWOC System," *IEEE Access*, vol. 9, pp. 57064-57074, 2021. DOI: [10.1109/ACCESS.2021.3071467](https://doi.org/10.1109/ACCESS.2021.3071467)
- [12] B. Wang, X. Tan, Z. Li, S. Li, M. Ma, and X. Zhang, "Simulation of underwater optical communication channel based on blue-green laser," *Proc. 2nd International Conference on Laser, Optics and Optoelectronic Technology (LOPET 2022)*, vol. 12343, 123431T, Oct. 2022. DOI: [10.1117/12.2649571](https://doi.org/10.1117/12.2649571)
- [13] J. Nie, L. Tian, S. Yue, Z. Zhang, and H. Yang, "Advanced beam shaping for enhanced underwater wireless optical communication," *Proc. Optical Fiber Communication Conference (OFC)*, W6A.24, Mar. 2021 DOI: [10.1364/OFC.2021.W6A.24](https://doi.org/10.1364/OFC.2021.W6A.24)
- [14] D. Jiang, X. Liu, Z. Hu, B. Zhu, Q. Zeng, and K. Qin, "Average irradiance with boresight pointing errors for flat-topped beam under atmospheric turbulence," *Optics Communications*, vol. 522, Nov. 2022. DOI: [10.1016/j.optcom.2022.128703](https://doi.org/10.1016/j.optcom.2022.128703)
- [15] M. Yousefi, F. D. Kashani, S. Golmohammady, and A. Mashal, "Scintillation and bit error rate analysis of a phase-locked partially coherent flat-topped array laser beam in oceanic turbulence," *Journal of the Optical Society of America A*, vol. 34, no. 12, pp. 2126-2137, 2017. DOI: [10.1364/JOSAA.34.002126](https://doi.org/10.1364/JOSAA.34.002126)
- [16] M. Zhao, X. Li, X. Chen, Z. Tong, W. Lyu, Z. Zhang, and J. Xu, "Long-reach underwater wireless optical communication with relaxed link alignment enabled by optical combination and arrayed sensitive receivers," *Optics Express*, vol. 28, no. 23, pp. 34450-34460, Nov. 2020. DOI: [10.1364/OE.410026](https://doi.org/10.1364/OE.410026)